Eur. Phys. J. E (2013) **36**: 111
DOI 10.1140/epje/i2013-13111-3

THE EUROPEAN PHYSICAL JOURNAL E

Regular Article

Self-assembly and gelation properties of glycine/leucine Fmoc-dipeptides*

Claire Tang[1,2], Rein V. Ulijn[3], and Alberto Saiani[1,a]

[1] School of Materials, The University of Manchester, Grosvenor Street, Manchester, M1 7HS, UK
[2] Manchester Institute of Biotechnology (MIB), The University of Manchester, 131 Princess Street, Manchester, M1 7DN, UK
[3] WestCHEM, Department of Pure & Applied Chemistry, University of Strathclyde, Thomas Graham Building, 295 Cathedral Street, Glasgow G1 1XL, UK

Received 28 March 2013 and Received in final form 3 July 2013
Published online: 3 October 2013

Abstract. Self-assembly of aromatic peptide amphiphiles is known to be driven by a combination of π-π stacking of the aromatic moieties and hydrogen bonding between the peptide backbones, with possible stabilisation from the amino acid side chains. Phenylalanine-based Fmoc-dipeptides have previously been reported for their characteristic apparent pK_a transitions, which were shown to coincide with significant structural and morphological changes that were peptide sequence dependent. Here, phenylalanine was replaced by leucine and the effect on the self-assembling behaviour of Fmoc-dipeptides was measured using potentiometry, fluorescence and infrared spectroscopy, transmission electron microscopy, X-ray scattering and shear rheometry. This study provides additional cues towards the elucidation of the sequence-structure relationship in self-assembling aromatic peptide amphiphiles.

1 Introduction

Self-assembling peptides attract significant interest due to the variety of supramolecular nanostructures that can be generated from them and their resulting potential applications [1,2]. These materials utilise peptides as versatile building blocks of choice whose constitutive amino acids offer a diverse range of functionalities and structures.

Numerous examples of peptides self-assembling via a combination of hydrophobic and/or π-π interactions as well as hydrogen bonding have been reported in the literature. For instance, the self-assembly of short peptides can be facilitated by coupling the peptidic components to terminal hydrophobic groups such as aliphatic chains [3] or aromatic ligands such as benzyloxycarbonyl (Cbz), naphthalene (Nap) or 9-fluorenylmethoxycarbonyl (Fmoc) [4]. The main challenge in this field is to develop an in-depth understanding of the correlation existing between peptide primary structure and self-assembly structure formed so as to be able to control the properties of the material formed.

We have recently proposed that the main driving force behind the self-assembly process of Fmoc-dipeptides constituted of phenylalanine residues is the aromatic π-π interactions of the fluorenyl moieties whilst hydrogen bonding has a secondary role [5]. However other studies suggest that the hydrophobicity of the compounds might also play an important part. In order to measure the impact of the aromatic side chains on the self-assembling behaviour of Fmoc-dipeptides, phenylalanine can be replaced by leucine, the alkyl side chain of which has a similar hydrophobicity as the phenyl side chain of phenylalanine [6]. Such type of substitution has previously been shown not to alter the ability of the molecules to self-assemble into higher-order structures [7]. Additionally, formation of hydrogels from leucine-based Fmoc-peptides by *p*H adjustment or by enzymatic reaction has been reported in the literature. Under specific conditions, Fmoc-LG was found to generate fibrillar networks forming hydrogels, whether the *p*H was adjusted with hydrochloric acid (HCl) [8] or sugar precursors of acid [9]. Fmoc-L_3 and Fmoc-L_5 self-assembly has also been observed following reverse hydrolysis [10]. Another example is that of the formation of hydrogels from Fmoc-LL via hydrolysis of the corresponding ester. Interestingly, distinct morphologies (nanotubes or nanofibres) were obtained depending on the route used to arrive at the Fmoc-LL gelator [11]. On the contrary, no hydrogels were formed from Fmoc-GL [8,12].

* Supplementary material in the form of a pdf file available from the Journal web page at
http://dx.doi.org/10.1140/epje/i2013-13111-3

[a] e-mail: a.saiani@manchester.ac.uk

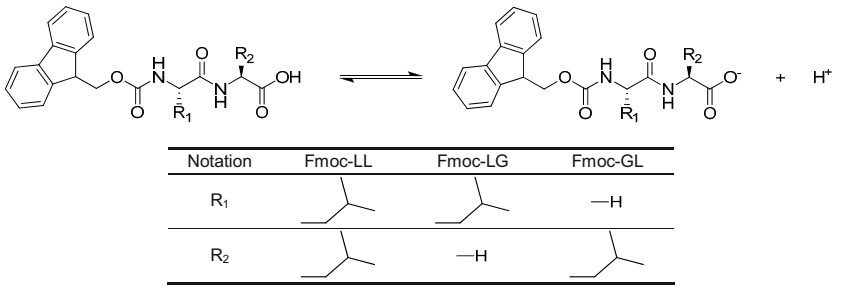

Fig. 1. Equilibrium between Fmoc-dipeptide neutral (acid) and ionised (conjugated base) forms and notation.

Fmoc-dipeptides based on combinations of phenylalanine and glycine were formerly shown to exhibit dramatic pK_a shifts that were related to significant structural modifications [5,13]. The main aim of the present work was to investigate the role played by the phenyl ring side chain (phenylalanine) in the self-assembly of these peptides by replacing it by an isobutyl chain (leucine) with a similar hydrophobicity. For this purpose employing the previously reported *p*H controlled procedure we herein present the study of leucine-based Fmoc-dipeptide homologues, Fmoc-LL, Fmoc-LG and Fmoc-GL (fig. 1). The systems were titrated by potentiometry, whilst the supramolecular interactions underpinning self-assembly were investigated using fluorescence and infrared spectroscopy. The morphology of the structures formed was characterised by transmission electron microscopy and X-ray scattering. Finally, the dynamic mechanical properties were studied using shear rheometry.

2 Materials and methods

Materials: All Fmoc-dipeptides were purchased from C S Bio Company (Menlo Park, USA) and used without further purification. The purity of the compounds was verified by HPLC (> 98%) and mass spectrometry. HPLC grade water and deuterated water (99.9 atom% D) were purchased from Merck and Sigma-Aldrich, respectively.

Sample preparation: Depending on the desired concentration, the required amount of Fmoc-dipeptide was suspended into 2 mL of HPLC grade water. Sodium hydroxide (0.5 M) was gradually added to the aqueous suspensions of Fmoc-dipeptide until *p*H 10.5 was reached ($\sim$ 55 μL for 10 mmol L^{-1} sample). The samples were vortexed and sonicated for one minute to fully dissolve the peptide amphiphiles. Depending on the concentration and on the target *p*H, a required volume of dilute hydrochloric acid (0.085 M) was then added dropwise while the solution was vortexed and sonicated until the target *p*H was obtained. Next, the samples were heated to 75–80 °C until fully dissolved (1.0, 2.5 and 1.5 minutes for Fmoc-LL, Fmoc-LG and Fmoc-GL, respectively) and homogenised. The samples were subsequently cooled and maintained at 4 °C for $\sim$ 12 hours (overnight) to promote or maintain gelation. To allow comparison between the studied samples, all were investigated after this same aging time. Reported *p*H values were those measured after storage. They were found to be identical to the *p*H values measured before heating within $\pm$0.3 units.

Potentiometry: *p*H measurements were performed using a Hanna Instruments *p*H210 *p*H-meter equipped with a Hamilton Spintrode *p*H-probe (reference system: Ag/AgCl, electrolyte: 3 M KCl, diaphragm: ceramic, sensitivity: 58 mV/*p*H unit at 25 °C). The *p*H-meter was calibrated before each experiment to check the response of the electrode with two buffer solutions purchased from Fisher Scientific: phthalate *p*H 4.01 and phosphate *p*H 7.01 buffer solutions.

"Titration" experiments: The 5, 10 and 20 mmol L^{-1} samples at *p*H 10.5 were prepared as described above. For 1 mmol L^{-1} samples, 5 mmol L^{-1} samples at *p*H 10.5 were used as stock solutions and diluted to the desired concentration in a final volume of 2 mL. The *p*H of the final solutions was then adjusted to *p*H 10.5. The "titration" experiments were performed by stepwise addition of small volumes of diluted HCl (0.085 M; 2–60 μL depending on *p*H and system), up to a total added volume of 750 μL. After each addition the samples were heated to 75–80 °C for one minute, vortexed, sonicated, and subsequently cooled back to room temperature using a water bath. *p*H values were recorded before and after heating of the samples. The samples were deemed fully mixed when no significant difference ($\pm$0.3 *p*H unit) was observed between two *p*H measurements. Due to the strong and constant agitation applied, samples were liquid at all times during the "titration" experiments. As a control, water was also titrated using the same methodology described above; that is, NaOH was added to the water in order to bring the *p*H of the solution to 10.5 and then HCl was added stepwise. Experiments, including the characterisation experiments described below, were repeated a least 3 times to ensure reproducibility.

Fluorescence spectroscopy: Fluorimetry experiments were undertaken using a Perkin-Elmer LS55 luminescence spectrometer equipped with a Julabo F25 temperature control device. After their preparation, the samples were transferred into PMMA disposable cuvettes (Fisher Scientific) with a path length of 1 cm and kept at 4 °C

overnight. Emission and excitation slit widths were set at 3 and 10 nm, respectively. Emission spectra (excitation at 265 nm) were acquired at 25 °C in the 300–600 nm range with a scan speed of 300 nm min^{-1} using FL WinLab software. Changes in the *p*H conditions and therefore in the self-assembled structures formed are likely to modify the refractive index of the samples and the quenching effect resulting from self-assembly. These effects would have a direct effect on the intensity of the transmitted light hence on the emission peaks' intensity. For this reason, fluorescence spectra were all normalised as a function of their respective maximum emission peak. The un-normalised spectra are presented in the supplementary material.

Fourier-transform infrared spectroscopy (FTIR): Multiple bounce attenuated total reflectance (ATR) FTIR experiments were undertaken using samples prepared in deuterated water. Spectra were recorded on a Thermo Nicolet 5700 spectrometer equipped with a trough plate comprising of a zinc selenide crystal, which permitted 12 reflections with a 45° angle of incidence. The samples were spread directly on the surface of the trough plate. Spectra were acquired in the 4000–400 cm^{-1} range with a resolution of 4 cm^{-1} over 128 scans. The deuterated water spectrum was used as background and subtracted from all spectra (software used: Omnic version 7.2, Thermo Electron Corporation).

Mechanical properties: Mechanical properties were assessed using a stress-controlled rheometer (Bohlin C-VOR) equipped with a Peltier device (Bohlin Instruments) to control temperature using a parallel-plate geometry (40 mm diameter). To ensure the measurements were made in the linear regime, amplitude sweeps were performed and showed no variation in G' and G'' up to a strain of 1%. The dynamic moduli of the hydrogel were measured as a function of frequency in the range 0.01–100 rad s^{-1} with a strain of 1%. To keep the sample hydrated, a solvent trap was used and the atmosphere within the sample chamber was saturated with water. Unless otherwise stated the experiments were performed at 25 °C and repeated at least three times (each time on new samples) to ensure reproducibility. The standard deviation of multiple experiments is represented by error bars in the dynamic frequency sweeps.

Transmission electron microscopy (TEM) and image analysis: A carbon-coated copper grid (400 mesh, Agar Scientific) was glow discharged for 30 seconds then placed on 10 μL of sample for 15 seconds. After blotting on Whatman 50 filter paper, the loaded grid was washed in double distilled water for 30 seconds and blotted. The sample was then stained with 10 μL of 2% (w/v) uranyl acetate (centrifuged for 5 minutes beforehand) for one minute and blotted for 10 seconds. Data were collected at high vacuum on a JEOL 1220 transmission electron microscope connected to a high resolution (up to 3 Å/pixel resolution) Gatan Orius CCD camera.

Wide angle X-ray scattering (WAXS): Wide angle X-ray scattering experiments were conducted using 10 mmol L^{-1} samples. Wet samples were spread onto glass slides as thin films and allowed to air dry for 48 hours prior to data collection. Experiments were performed on a Philips X'Pert diffractometer equipped with a copper source (wavelength of 1.54 Å), applying scans from Bragg angles of 1° to 33°. The glass slide spectrum was used as background and subtracted from all spectra.

3 Results and discussion

3.1 "Titrations"

"Titration" experiments previously revealed that Fmoc-dipeptides were characterised by substantially shifted apparent pK_a transitions with respect to their theoretical pK_a value[1] that coincided with structural transitions. Fmoc-FF exhibited two distinct pK_a transitions that were shown to be related to the structural transition of fibrils into tape-like structures that precipitated at low *p*H ($< pK_a$ 2) [13]. In contrast, systems such as Fmoc-FG, Fmoc-GG and Fmoc-GF for instance displayed a single apparent pK_a transition [5]. Fmoc-LL, Fmoc-LG and Fmoc-GL were titrated at concentrations of 1, 5, 10 and 20 mmol L^{-1} using the previously described procedure [5, 13]. For all "titrations" the peptide amphiphiles were first dissolved by raising the *p*H to 10.5 with NaOH. HCl was then added and variation of the samples' *p*H was measured as shown in figs. 2A–C. The same procedure was applied to water as a control.

At *p*H 10.5, Fmoc-LL was fully dissolved at all concentrations studied and clear solutions were obtained. As shown in fig. 2A, the *p*H of all solutions progressively decreased upon addition of HCl. A transition was observed at *p*H values of 8.5, 7.6, 7.4 and 6.4 for the 20, 10, 5 and 1 mmol L^{-1} samples, respectively, and the specimen started to become cloudy. After the transition, the *p*H started to drop again for all the samples. An increase in turbidity was observed in particular for 10 and 20 mmol L^{-1} samples, which became more viscous. As observed in our former studies [5,13], the *p*H of the 20 mmol L^{-1} sample was found to rise slightly before dropping again. This feature was reproducible and also observed for 30 mmol L^{-1} samples (data not shown), and is thought to be related to the initial nucleation of the self-assembly process. Upon further addition of HCl, decrease in *p*H was accompanied by the formation of a precipitate. At *p*H $\sim$ 2.1, phase separation occurred with the emergence of a clear liquid phase at the top and a precipitate at the bottom of the test tube and the "titration" curves started to merge with the water curve [5].

For all concentrations investigated, Fmoc-LG peptides fully dissolved at *p*H 10.5 following addition of NaOH. The *p*H of the solutions was then gradually lowered as HCl was added (fig. 2B). For 20, 10 and 5 mmol L^{-1} samples, *p*H

[1] Theoretical pK_a values were calculated using SPARC web calculator on `http://archemcalc.com/sparc`.

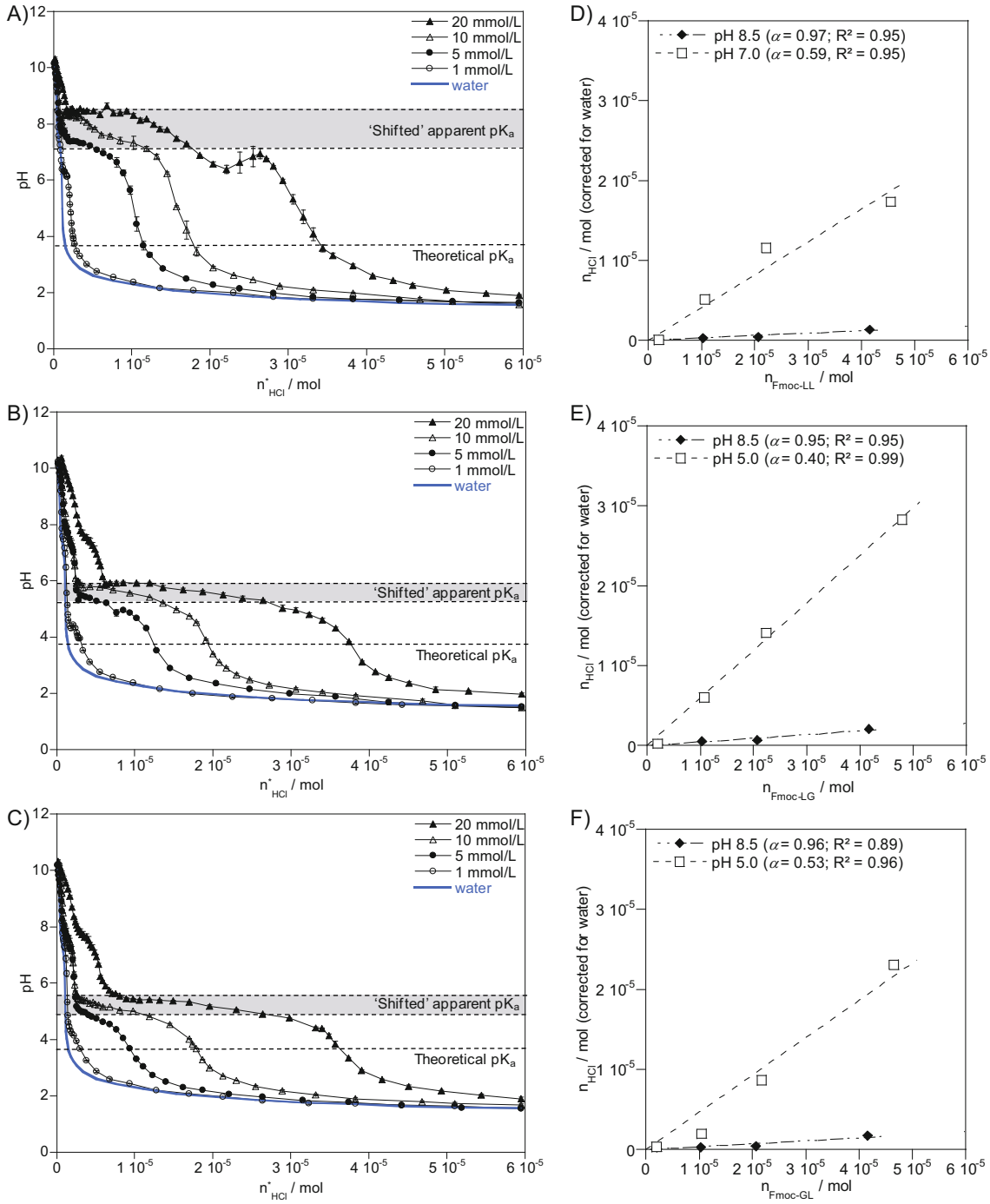

Fig. 2. "Titration" curves (*p*H *vs.* moles of added HCl) of water and A) Fmoc-LL, B) Fmoc-LG and C) Fmoc-GL samples at 1, 5, 10 and 20 mmol L^{-1}. n_{HCl} (moles of HCl added corrected for moles of HCl needed to titrate water) *vs.* $n_{Fmoc\text{-}dipeptide\text{-}COOH}$ (moles of Fmoc-dipeptide present in the sample) for the 1, 5, 10 and 20 mmol L^{-1} samples of D) Fmoc-LL at *p*H values of 8.5 and 7.0, E) Fmoc-LG at *p*H values of 8.5 and 5.0 and F) Fmoc-GL at *p*H values of 8.5 and 5.0. (α: degree of ionisation derived from the slope of the fitted linear curves.)

transitions occurred at values of 5.9, 5.8 and 5.3, respectively, whilst the samples became cloudy. The turbidity of the samples increased along the transition and was found to be more apparent for the most concentrated samples (10 and 20 mmol L^{-1}). After the transition, the samples' *p*H decreased again while precipitation occurred at *p*H $\sim$ 3.0 for 20, 10 and 5 mmol L^{-1} samples. At 1 mmol L^{-1} the solution remained clear throughout the experiment, although a transition was observed at lower *p*H value of $\sim$ 4.4. As the *p*H decreased further all the "titration" curves started to merge with the control curve.

Fmoc-GL followed the same overall trend as Fmoc-LG. At *p*H 10.5 the peptide amphiphiles were found to be soluble at all concentrations studied. A decrease in the

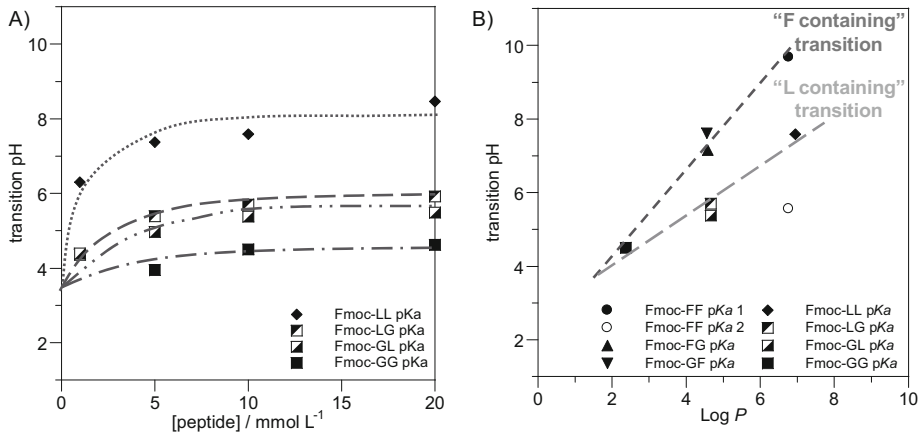

Fig. 3. A) Transition pH values *versus* concentration of Fmoc-LL, Fmoc-LG and Fmoc-GL at 1, 5, 10 and 20 mmol L $^{-1}$. B) Transition pH values *versus* $\log P$ values of the Fmoc-dipeptides at 10 mmol $^{-1}$. Data taken from ref. [13] for Fmoc-FF and from ref. [5] for Fmoc-FG, Fmoc-GG and Fmoc-GF.

samples' pH (fig. 2C) and an increase in their turbidity were observed upon addition of HCl. Transitions were observed at pH values of 5.4, 5.1, 5.0 and 4.3 for 20, 10, 5 and 1 mmol L^{-1} samples, respectively. Once the transition was complete the samples' pH dropped again. However as the samples precipitated in the form of a solid mass constituted of insoluble peptide amphiphiles, they became less turbid. Towards the end of the "titrations" the liquid phase became almost clear at all concentrations tested and the samples' curves were found to merge with the water curve.

As opposed to Fmoc-FF but similar to Fmoc-FG, Fmoc-GG and Fmoc-GF only one apparent pK_a transition was observed for Fmoc-LL, Fmoc-LG and Fmoc-GL. The degree of ionisation, α, of this set of peptide amphiphiles was estimated as previously for the phenylalanine-based Fmoc-dipeptides [5,13]. Figures 2D–F show the degree of ionisation of the three Fmoc-dipeptides above and below their respective apparent pK_a that is at pH 8.5 and 7.0 for Fmoc-LL and pH 8.5 and 5.0 for Fmoc-LG and Fmoc-GL. n_{HCl} was plotted against $n_{\text{Fmoc-dipeptide-COOH}}$ at each stage and α was inferred from the slope of the fitted linear curves. Before the transition arose (pH 8.5), 97%, 95% and 96% of Fmoc-LL, Fmoc-LG and Fmoc-GL, respectively, were in their ionised form. Neutralisation of the molecules just started during the pK_a transition and continued as the pH was decreased further as about half of them were still in their ionised form just below their apparent pK_a (59%, 40% and 53% of Fmoc-LL, Fmoc-LG and Fmoc-GL, respectively).

The apparent pK_a transitions were found to be dependent upon increasing the concentrations of the peptide amphiphiles up to 5–10 mmol L^{-1} (fig. 3A). Above this critical value, further increase in peptide concentration did not have any effect on the pH values at which the pK_a transitions occurred. The pK_a transitions of the Fmoc-dipeptides were all shifted towards higher values compared to their theoretical pK_a^{th}, as recently reported in the literature for similar systems [14]. Fmoc-LL ($pK_a^{\mathrm{th}} = 3.79$), Fmoc-LG ($pK_a^{\mathrm{th}} = 3.82$) and Fmoc-GL ($pK_a^{\mathrm{th}} = 3.79$) displayed pK_a shifts of about 4.3, 2.0 and 1.5 pH units on average, respectively, at 10 mmol L^{-1}. Such behaviour is not uncommon since dramatic pK_a shifts have been reported for self-assembling proteins and peptide amphiphiles in hydrophobic environments, [15,16] fatty acid soaps, [17,18] and ribonucleases [19]. It could either result from the destabilisation and reduced ability of the carboxylate groups to create hydrogen bonds in hydrophobic environments or from the self-assembly of ionised with un-ionised species, as suggested by the ionisation levels obtained in our investigation on Fmoc-FF [13]. As previously shown, the apparent pK_a transition values were shown to correlate with the hydrophobicity ($\log P$) of the Fmoc-dipeptide molecules [5,14]. The shifted pK_a values were found to arise at high pH for molecules possessing high $\log P$ values[2] (*e.g.* Fmoc-LL) and at lower pH for molecules characterised by lower $\log P$ values (*e.g.* Fmoc-GL) (fig. 3B). Although the carboxylic acid group in free leucine is characterised by a higher pK_a than in free phenylalanine, the pK_a transitions for the leucine-based Fmoc-dipeptides were found to occur at lower pH than for their phenylalanine-based homologues, suggesting an effect of the side chain nature (aliphatic or aromatic) on the transition pH.

Due to the slight increase in pH observed below the apparent pK_a transition for Fmoc-LL at 20 mmol L^{-1}, the pH drop following the pK_a transition was found to be gradual but did not reveal a two-transition feature as shown by Fmoc-FF [13]. Like Fmoc-FG, [5] Fmoc-LG self-assembly process was associated with a single pH transition. As for Fmoc-GF, no hydrogels were formed from Fmoc-GL under all pH conditions tested. Additionally, clearer solutions rather than turbid mixtures were obtained from Fmoc-GL upon lowering pH above and below the apparent pK_a. This paper will therefore not focus on the characterisation of this system. In the following sections the ionisation behaviour of Fmoc-LL and Fmoc-LG

[2] $\log P$ values were determined using ACD/Labs v. 12.01/ ChemSketch.

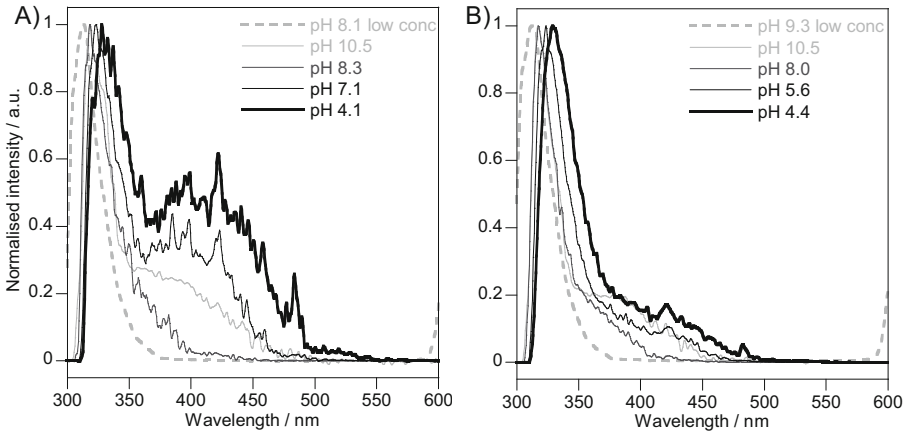

Fig. 4. Normalised fluorescence emission spectra of A) Fmoc-LL and B) Fmoc-LG samples at 10 mmol L^{-1} at *p*H 10.5 starting point of the "titration" experiments and at different *p*H values above and below their respective apparent pK_a and at low concentration (0.1 mmol L^{-1}) above their apparent pK_a (dotted lines).

will be related to the self-assembly and gelation properties of the systems as a function of *p*H using structural and spectroscopic characterisation techniques.

3.2 Supramolecular interactions

The behaviour in solution of the leucine-based Fmoc-dipeptides revealed similarities with what was observed for phenylalanine-based Fmoc-dipeptides since the *p*H at which the pK_a transition occurred increased with the hydrophobicity of the molecules.

The results of our recent study suggested that the main driving force behind the self-assembly process of phenylalanine-based Fmoc-dipeptides was the hydrophobic π-π interactions of the fluorenyl moieties [5]. In some of these peptides, the phenyl rings of the amino acids side chains were found to participate in the intermolecular interactions between phenylalanine-based Fmoc-dipeptides. In order to assess whether the peptide amphiphiles π-stacked in a different manner due to the lack of aromatic moieties in leucine-based Fmoc-dipeptides or if the alkyl chains were likely to interfere in the overlapping of the Fmoc groups, fluorescence spectroscopy was used to monitor the environment of the Fmoc-LL and Fmoc-LG fluorenyl moieties. Measurements were carried out on 10 mmol L^{-1} samples as a function of *p*H and at 0.1 mmol L^{-1} at *p*H $\sim$ 8.6. All the fluorescence spectra were normalised so that the intensity of the emission maximum was set to 1 (see fig. S1 of supplementary material for the non-normalised spectra). As shown in fig. 4, the two systems of interest displayed common features.

At low concentration (0.1 mmol L^{-1}) and above the apparent pK_a (*p*H $\sim$ 8.6) of both Fmoc-dipeptides studied, clear solutions were obtained. In these conditions all molecules should be in their ionised form. Hence the emission maximum observed at $\sim$ 313 nm for all samples was ascribed to the fluorenyl fluorescence of Fmoc-dipeptide monomers (fig. 4, dotted lines).

At 10 mmol L^{-1} (*i.e.* above the critical gelation concentration of the two systems) an emission maximum presumably related to antiparallel Fmoc excimers was observed at 317–330 nm at all *p*H conditions tested. The presence of this peak at *p*H 10.5 indicated that interactions between the Fmoc-dipeptides occurred even at high *p*H, forming base dimer units, probably at the origin of the structures formed at lower *p*H. As the *p*H was reduced this band was found to shift from 317 nm towards 330 nm for Fmoc-LL and Fmoc-LG, showing that the Fmoc groups constituting the dimers were overlapping in a more efficient manner [5].

A shoulder centred at 370–375 nm likely indicative of Fmoc excimers arranged in a parallel manner [20,21], possibly within micellar assemblies [22], was also detected. This band was found to be particularly pronounced at *p*H 10.5 than at any other *p*H conditions tested. The shoulder ascribed to parallel dimers was no longer observed at lower *p*H. This feature could be due to fibrillar self-assembly occurring at lower *p*H, which is likely to lock the molecules into antiparallel arrangements within the supramolecular structures as will be described in the following section. Interestingly, this shoulder was found to be overall more marked for the leucine-based Fmoc-dipeptides than for Fmoc-FF [5]. This behaviour is in agreement with the effect of the molecular flexibility on parallel dimerisation since the leucine aliphatic side chain confers more flexibility to the molecule tail than the phenyl ring of the phenylalanine side chain.

An extensive emission band was observed at $\sim$ 421 nm at or below *p*H values of 7.1 and 5.6 for Fmoc-LL and Fmoc-LG, respectively, which is in both cases below the apparent pK_a transition. As previously mentioned, this photoluminescence peak is characteristic of the π-π stacking of multiple fluorenyl moieties and indicates the presence of higher-order aggregates [21]. This behaviour is consistent with the hypothesis that self-assembled structures are formed below the shifted pK_a. As shown in fig. 4A), the photoluminescence emission was particularly intense for Fmoc-LL. Detection of a photoluminescence band in these conditions implies that the fluorenyl groups could be packed in hydrophobic clusters away from the solvent in the aggregates formed [23].

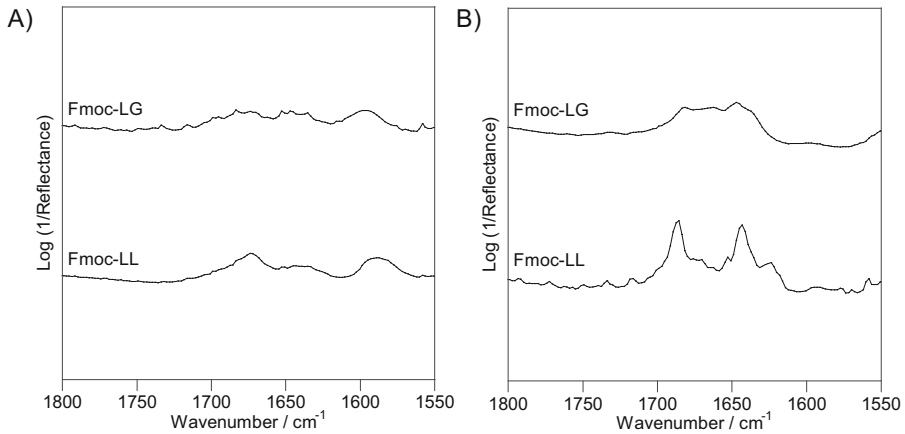

Fig. 5. FTIR spectra of Fmoc-dipeptide samples at 10 mmol L^{-1} prepared in D_2O. A) above the apparent pK_a (at pH 8.1 and 7.5 for Fmoc-LL and Fmoc-LG, respectively) and B) below the apparent pK_a (at pH 6.8 and 5.5 for Fmoc-LL and Fmoc-LG, respectively).

The fluorescence study of leucine-based Fmoc-dipeptides revealed that, like in phenylalanine-based Fmoc-dipeptides, the fluorenyl moieties were preferentially arranged in an antiparallel fashion at lower pH. However at high pH, when molecules are mainly ionised, parallel arrangements can also be found. Again, lowering the pH appeared to enhance the overlapping of the Fmoc-LL and Fmoc-LG molecules, possibly due to the presence of fewer ionised entities in solution causing fewer electrostatic repulsions and hence favouring the formation of higher-order aggregates.

Due to the absence of bulky phenyl side group in leucine, inclusion of this amino acid in Fmoc-dipeptides should result in the enhancement of the overall flexibility of the molecules and therefore affect the conformation adopted by the peptide component. However like phenylalanine, leucine is known to favour the formation of β-sheets [24]. In order to verify the conformation adopted by the peptidic tail of Fmoc-LL and Fmoc-LG the two systems were studied by FTIR. As shown in fig. 5A, in both cases no evidence of β-sheet formation was observed above the respective apparent pK_a of the Fmoc-dipeptides. In contrast, below the apparent pK_a bands at 1687 and 1624 cm^{-1} characteristic of β-sheets were detected in the amide I region for Fmoc-LL (fig. 5B), which is in agreement with the results of Das *et al.* [11]. In addition, the peak at 1643 cm^{-1} showed the coexistence of unordered structures. The presence of phenylalanine beside the fluorenyl moiety in Fmoc-FF and Fmoc-FG was previously found to provide certain rigidity to the peptide backbone of the molecules, allowing them to form β-sheet structures [5]. Despite the absence of such aromatic group β-sheet conformation was detected for Fmoc-LL under specific conditions. Although no distinct evidence of β-sheet formation was identified for Fmoc-LG below the apparent pK_a (fig. 5B), from the bands detected in the amide I region of the infrared spectrum it is clear that the system went through a transition. This behaviour is likely due to a different type of molecular interactions forming below the apparent pK_a, which could be associated with structural changes. As demonstrated by fluorescence spectroscopy and as will be confirmed below by TEM, the formation of self-assembled structures is independent of β-sheet formation, which is in agreement with the results of our previous investigation [5].

It can also be noted that, for both Fmoc-LL and Fmoc-LG, an infrared absorption band at $\sim$ 1596 cm^{-1}, characteristic of carboxylate groups, was detected above their respective apparent pK_a, confirming the ionised state of the molecules.

As suggested by fluorescence and infrared spectroscopy, the formation of organised self-assembled structures occurred upon lowering pH. In order to verify whether the one-transition feature displayed by this set of Fmoc-dipeptides was related to structural transitions and gelation of the systems, the mechanical properties of the samples were assessed using shear rheometry and the systems were characterised as a function of pH using TEM and WAXS.

3.3 Morphology and mechanical properties

Clear solutions were obtained from Fmoc-LL above the apparent pK_a. The liquid nature of the sample was confirmed by shear rheometry. As illustrated in fig. 6A at pH 8.5, the elastic modulus G' was found to be lower than the viscous modulus G'' until a crossover of the moduli was observed at around 10 rad s^{-1}. Both G' and G'' showed strong frequency dependence between 0.01 and 100 rad s^{-1}, which is indicative of liquid-like materials. As shown by TEM (fig. 7A), self-assembly did not occur in these pH conditions, which was consistent with the absence of Bragg peaks on the WAXS pattern at pH 8.2 (fig. 8A).

Below the apparent pK_a, translucent self-supported hydrogels were formed. As can be seen from fig. 6A at pH 7.0, G' was higher than G'' between 0.01 and 100 rad s^{-1}, with both moduli displaying weak frequency

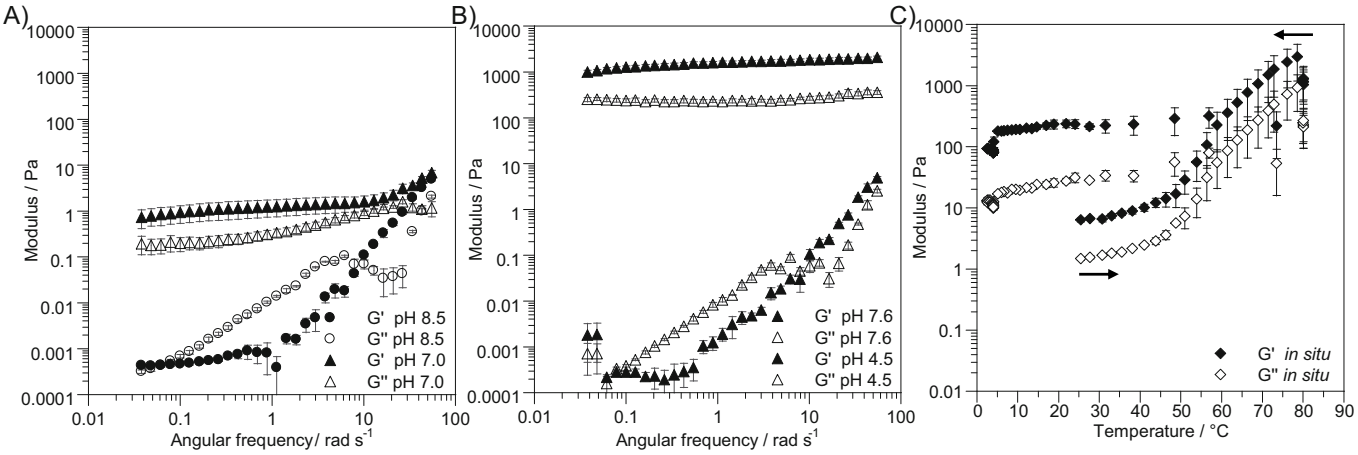

Fig. 6. A) Dynamic frequency sweep of Fmoc-LL sample (10 mmol L^{-1}) at *p*H 8.5 and 7.0 (above and below the apparent, respectively). B) Dynamic frequency sweep of Fmoc-LG sample (10 mmol L^{-1}) at *p*H 7.6 and 4.5 (above and below the apparent, respectively). C) Dynamic temperature sweep of Fmoc-LG samples (10 mmol L^{-1}) from 25 °C to 80 °C to 4 °C.

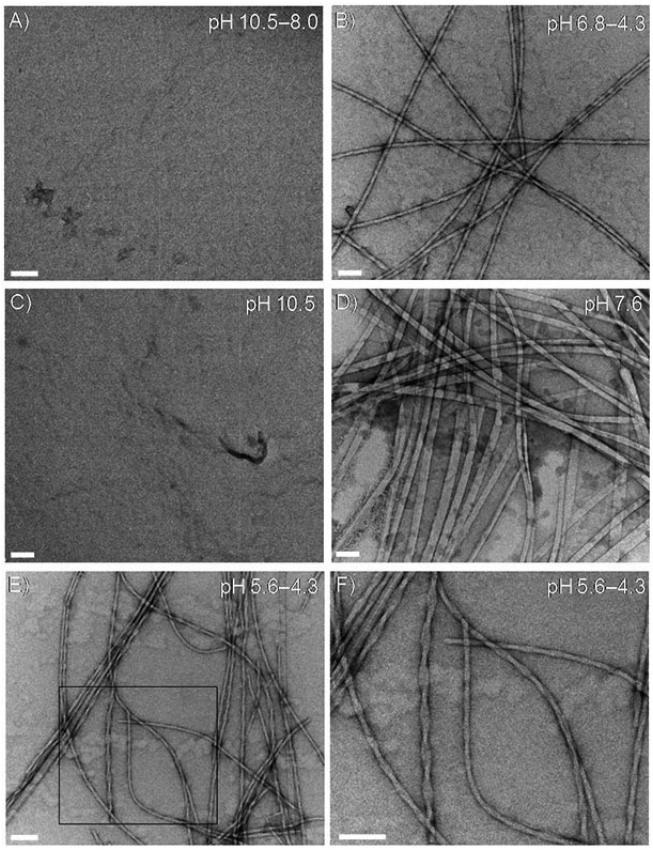

Fig. 7. TEM micrographs of Fmoc-dipeptide samples at 10 mmol L^{-1}. A) Fmoc-LL at *p*H 10.5 (starting point of the "titration" experiments) and above the apparent pK_a, B) Fmoc-LL below the apparent pK_a, C) Fmoc-LG at *p*H 10.5, D) Fmoc-LG above the apparent pK_a, E) Fmoc-LG below the apparent pK_a and F) close up of the box in E). Scale bars represent 100 nm.

dependence, confirming the gel-like nature of the sample. G' values were in the range of 0.7–5 Pa, showing that the hydrogels formed by Fmoc-LL were weak. The entangled fibrillar network observed by TEM at *p*H 6.8 was in agreement with the rheological behaviour of the system. As can be seen in fig. 7B, fibres of $\sim 15.7 \pm 0.7$ nm in width were formed. A topology of this type with a comparable size has been reported for Fmoc-LL hydrogels formed through hydrolysis of the corresponding ester. Das *et al.* showed that the morphology and dimensions of the self-assembled structures obtained varied depending on the route via which they were prepared. Tubular (15.2±1.1 nm in width) and fibrillar (12.0 ± 2.5 nm in width) structures were generated when the corresponding ester was synthesised by conventional solution phase methodology and by solid-solid reactions, respectively [11]. As shown by WAXS in fig. 8A, broad reflection peaks were detected at 4.1, 5.3 and 7.2 nm^{-1}, corresponding to distance of 15.4, 11.9 and 8.7 Å. These Bragg peaks indicated that the structures formed did not result from lateral self-assembly, hence no lamellar organisation was observed. Although FTIR data suggested that Fmoc-LL peptide tail adopted a β-sheet conformation, no reflection peak characteristic of the spacing between β-strands was detected at a distance of 4.3 Å, as was observed previously for Fmoc-FF [13].

When the *p*H was reduced to 4.3, milky flocculates suggesting the formation of insoluble self-assembled structures were obtained. As shown in fig. 7B, nanofibres were still observed by TEM. The WAXS pattern in fig. 8A displayed a drop in intensity indicating a loss of structure that was probably induced by the precipitate state of the samples.

Although leucine and phenylalanine have comparable hydrophobicities, Fmoc-LL and Fmoc-FF [13] showed different behaviours. Fmoc-LL was characterised by a single pK_a transition. Hydrogels that were associated with

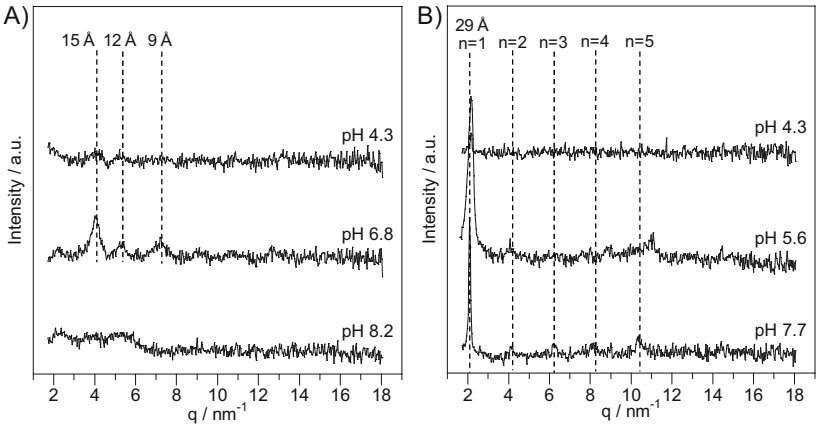

Fig. 8. WAXS spectra of Fmoc-dipeptide samples at 10 mmol L^{-1} dried: A) Fmoc-LL at *p*H 8.2 (above the apparent pK_a) and *p*H 6.8 and 4.3 (below the apparent pK_a) and B) Fmoc-LG at *p*H 7.7 and 5.6 (above the apparent pK_a) and *p*H 4.3 (below the apparent pK_a).

the presence of fibrillar networks on the microscopic scale were formed in both cases, however no lateral association of the fibres characteristic of a lamellar organisation was observed for Fmoc-LL.

Above the apparent pK_a, clear solutions were obtained from Fmoc-LG. As we can see from the frequency sweep in fig. 6B, G' was mainly lower than G'' at *p*H 7.6 and both moduli were frequency dependent between 0.01 and 100 rad s^{-1}, confirming that the material was liquid. However at *p*H 7.6 the presence of a small amount of precipitate was observed in the liquid sample, suggesting that most of the molecules were still in solution (fig. 5B). Relatively straight ribbons of 24.0 ± 1.7 nm in width were observed by TEM in a few windows of the grid (fig. 7D). These self-assembled structures were likely to constitute the precipitated fraction of the sample. As can be seen from the WAXS data at *p*H 7.7 (fig. 8B), a lamellar packing pattern with a *d* spacing of 29.0 Å ($q = 2.2\,nm^{-1}$) and up to five higher-order reflections was detected. This feature indicated that the straight ribbons observed by TEM resulted from the lateral association of fibrillar structures.

At *p*H $\sim$ 5.5 (below the apparent pK_a) viscous solutions were obtained. Twisted ribbons with average pitch and width of 149.2 ± 20.3 nm and 13.5 ± 0.9 nm, respectively, were observed on the TEM micrographs (figs. 7E–F). These structures were found to coexist with a few flat ribbons of 21.3 ± 1.0 nm in width, remaining from the previous *p*H stage. At this same *p*H, the reflection at 29.0 Å ($q = 2.2\,nm^{-1}$) corresponding to a periodic unit present in the straight ribbons was still detected, however the intensity of the five higher-order reflections was attenuated (fig. 8B). This attenuation could be due to the presence of the coexisting twisted ribbons.

As the *p*H was lowered further to $\sim$ 4.3, translucent hydrogels were formed. Like the previously studied Fmoc-FG hydrogels [5], these samples were found to gel (*i.e.* stop flowing upon inversion of the vial) during the heating step at 80 °C and to be relatively stable upon cooling to 4 °C and room temperature (should the gels have been completely formed at high temperature). As shown in fig. 6B, the gel-like nature of the sample was confirmed by rheology. G' values (1000–2080 Pa) were about one order of magnitude higher than G'' values and both moduli were slightly frequency dependent between 0.01 and 100 rad s^{-1}, which suggested the presence of an entangled fibrillar network. Higher values of G' have been reported for Fmoc-LG hydrogels obtained by *p*H change (5900 Pa) [9]. Such difference is likely to be related to the method of preparation of the samples. The entangled nature of the system was consistent with the type of microstructures observed by TEM as the presence of twisted ribbons, similar to those formed at *p*H $\sim$ 5.5, was noted (figs. 8E–F). The relative reduction of the proportion of flat ribbons compared to that of the twisted ribbons led to a significant decrease in intensity of the Bragg peak at $2.2\,nm^{-1}$ (*i.e.* $d = 29.0$ Å).

The Fmoc-LG and the Fmoc-FG [13] systems were characterised by common features. Both were found to form stable hydrogels upon heating and exhibited structural and morphological changes, including in supramolecular chirality, as the systems passed from solutions into gels (figs. 8D–F). For both peptide amphiphiles, the self-assembled structures did not exhibit any lamellar organisation. On the other hand, replacement of the phenylalanine by a leucine residue altered the relative rigidity of the molecule, preventing Fmoc-LG from creating intermolecular hydrogen bonding that would stabilise the structures into β-sheets. As a result, this conformation was not detected at any *p*H conditions.

The formation of stable hydrogel from Fmoc-LG was also found to be temperature dependent (in the same manner as Fmoc-FG, as previously reported [5]). The mechanical properties of the system were therefore monitored below the apparent pK_a (*p*H $\sim$ 4.7), as a function of temperature during *in situ* (in the rheometer) gel formation.

Sequential addition of NaOH and HCl was undertaken as described in the Materials and methods section. Following this the samples were not heated but thoroughly

sonicated. They were then subjected to the following temperature variations: the temperature was raised from 25 to 80 °C at a rate of 10 °C min^{-1}, maintained for 2.5 min at 80 °C, reduced from 80 to 4 °C over 1 min and kept for 8.5 min at 4 °C. The temperature-dependent mechanical spectrum of Fmoc-LG is presented in fig. 6C. G' values were found to be higher (about one order of magnitude) than the G'' values at all temperatures, including at room temperature (at the beginning of the experiment). This observation suggests that self-assembly occurred at 25 °C before the samples were heated. The lack of stiffness of the sample was however confirmed by the relatively low G' values displayed by the solutions between 25 and 50 °C. Both moduli increased by about three orders of magnitude as the temperature was risen further, reaching a maximum G' value of ~ 3000 Pa at 80 °C (*i.e.* close to the G' values obtained for the corresponding pre-formed gels). G' and G'' values were then found to decrease of about one order of magnitude ($G' \sim 320 \pm 65$ Pa) when the samples were kept at 80 °C and to remain relatively constant as the samples were cooled down between 70 and 4 °C. The heating-cooling sequence between 25 and 4 °C resulted in an overall increase of about one order of magnitude in both G' and G''. As observed for Fmoc-FG, Fmoc-LG preformed hydrogels displayed storage modulus values that were about ten times higher than those obtained for the systems heated *in situ*.

A TEM micrograph of a non-heated sample is shown in fig. S2 of the supplementary material. Although the microstructures formed from non-heated samples looked less regular than those obtained from heated samples (fig. 7E), the coexistence of twisted and flat ribbons was observed in both cases. The heating step was shown to improve the homogeneity of the samples without altering the topography of the self-assembled structures. The difference in mechanical properties between the heated and non-heated sample is therefore thought to be due to the formation of overall more homogeneous network topology when the samples are cooled down slowly in the rheometer. This results in the absence of large fibre aggregates that are known to reinforce the sample mechanical properties.

4 Conclusion

As previously observed for Fmoc-FG, Fmoc-GF and Fmoc-GG, the behaviour of Fmoc-LL, Fmoc-LG and Fmoc-GL upon titration revealed that each system was characterised by one apparent pK_a transition, which in all cases has been shown to be related to structural and morphological changes that were peptide sequence dependent.

Based on fluorescence spectroscopy data, Fmoc-LL and Fmoc-LG systems were found to be ordered through their Fmoc groups, which were mainly π-stacked into antiparallel dimers that were thought to correspond to the base unit of the self-assembled supramolecular structures generated as the *p*H was reduced. In addition the Fmoc-LL peptide tail was found to arrange in β-sheets below the apparent pK_a. The coexistence of unordered structures was also detected. As expected, Fmoc-LG did not form β-sheets in any conditions due to the flexibility of the molecules brought about by the glycine residue.

Although the Fmoc-LG molecules were ionised above the apparent pK_a straight ribbons were observed at the microscopic scale. Neutralisation of the peptide amphiphiles induced the formation of an entangled network of twisted ribbons. Stable hydrogels associated with this phenomenon were obtained upon heating. The self-assembly of Fmoc-LL into an entangled network of fibres of $\sim$ 15.7 nm in width also led to hydrogel formation, however the modulus values were lower than for Fmoc-LG gels. The absence of a regular scattering pattern — in agreement with the TEM observations— showed that only Fmoc-LG exhibited any lamellar organisation. The *d* spacings detected by WAXS were therefore ascribed to periodic units down the long axis of the structures rather than lateral association of fibres.

Similar behaviours were observed between the leucine-based Fmoc-dipeptides and their phenylalanine-based homologues [5]. Fmoc-LL, Fmoc-LG and Fmoc-GL peptide amphiphiles were each characterised by a single shifted pK_a transition. Study of the systems as a function of *p*H showed that this transition coincided with molecular self-assembly or structural and morphological changes. Again, the structural properties of the systems were found to be dependent on the peptide sequence. Entangled fibrillar networks associated with hydrogel formation were formed for Fmoc-LL and Fmoc-LG as observed for Fmoc-FF and Fmoc-FG. As previously reported for Fmoc-FG, Fmoc-LG gels were found to form upon heating.

We have shown in the present work that the replacement of the phenyl ring by an isobutyl chain in our dipeptide systems does not affect the propensity of the molecule to self-assemble into extended fibrillar structures clearly pointing toward the key role played by the Fmoc group and π-π interactions in driving the self-assembly of these systems. This work also confirmed that placing glycine just after the Fmoc group in these systems prevents self-assembly. This strongly suggests that the hydrophobicity and/or the rigidity of the molecule peptidic tail is an important parameter for self-assembly. Structural differences were observed by TEM and WAXS for the fibres formed showing that the replacement of the phenyl ring by an isobutyl chain does probably affect the packing of the molecules within the fibres. Overall this work contributes toward the establishment of design rules for the design of self-assembling peptide based materials using Fmoc-dipeptides.

The authors gratefully acknowledge the EPSRC and Leverhulme Trust for their financial support as well as Judith Shackleton and Paula Crook from the University of Manchester for their assistance with WAXS and FTIR measurements, respectively.

References

1. R. de la Rica, H. Matsui, Chem. Soc. Rev. **39**, 3499 (2010).
2. J.P. Jung, J.Z. Gasiorowski, J.H. Collier, Peptide Sci. **94**, 49 (2010).
3. H. Cui, M.J. Webber, S.I. Stupp, Peptide Sci. **94**, 1 (2010).
4. D.J. Adams, Macromol. Biosci. **11**, 160 (2011).
5. C. Tang, R.V. Ulijn, A. Saiani, Langmuir **27**, 14438 (2011).
6. O.D. Monera, T.J. Sereda, N.E. Zhou, C.M. Kay, R.S. Hodges, J. Peptide Sci. **1**, 319 (1995).
7. N.S. de Groot, T. Parella, F.X. Aviles, J. Vendrell, S. Ventura, Biophys. J. **92**, 1732 (2007).
8. V. Jayawarna, M. Ali, T.A. Jowitt, A.F. Miller, A. Saiani, J.E. Gough, R.V. Ulijn, Adv. Mater. **18**, 611 (2006).
9. D.J. Adams, M.F. Butler, W.J. Frith, M. Kirkland, L. Mullen, P. Sanderson, Soft Matter **5**, 1856 (2009).
10. R.J. Williams, A.M. Smith, R. Collins, N. Hodson, A.K. Das, R.V. Ulijn, Nat. Nanotechnol. **4**, 19 (2009).
11. A.K. Das, R.F. Collins, R.V. Ulijn, Small **4**, 279 (2008).
12. A.M. Smith, R.F. Collins, R.V. Ulijn, E. Blanch, J. Raman Spectrosc. **40**, 1093 (2009).
13. C. Tang, A.M. Smith, R.F. Collins, R.V. Ulijn, A. Saiani, Langmuir **25**, 9447 (2009).
14. D.J. Adams, L.M. Mullen, M. Berta, L. Chen, W.J. Frith, Soft Matter **6**, 1971 (2010).
15. D.W. Urry, S.Q. Peng, T.M. Parker, D.C. Gowda, R.D. Harris, Angew. Chem. Int. Ed. **32**, 1440 (1993).
16. K. Ariga, T. Nakanishi, J.P. Hill, M. Shirai, M. Okuno, T. Abe, J.-i. Kikuchi, J. Am. Chem. Soc. **127**, 12074 (2005).
17. J.R. Kanicky, A.F. Poniatowski, N.R. Mehta, D.O. Shah, Langmuir **16**, 172 (2000).
18. J.R. Kanicky, D.O. Shah, Langmuir **19**, 2034 (2003).
19. R.L. Thurlkill, G.R. Grimsley, J.M. Scholtz, C.N. Pace, J. Mol. Biol. **362**, 594 (2006).
20. D. Schweitzer, K.H. Hausser, M.W. Haenel, Chem. Phys. **29**, 181 (1978).
21. Z. Yang, H. Gu, Y. Zhang, L. Wang, B. Xu, Chem. Commun. **2**, 208 (2004).
22. J.W. Sadownik, J. Leckie, R.V. Ulijn, Chem. Commun. **47**, 728 (2011).
23. J.R. Lakowicz, *Principles of Fluorescence Spectroscopy*, 3rd edition (Springer, Boston, 2006).
24. P.Y. Chou, G.D. Fasman, Trends Biochem. Sci. **2**, 128 (1977).